

Structure of Crystals of Hard Colloidal Spheres

P. N. Pusey,⁽¹⁾ W. van Meegen,^(1,2) P. Bartlett,⁽³⁾ B. J. Ackerson,^(1,4)
J. G. Rarity,⁽¹⁾ and S. M. Underwood⁽²⁾

⁽¹⁾Royal Signals and Radar Establishment, Malvern, WR14 3PS, United Kingdom

⁽²⁾Department of Applied Physics, Royal Melbourne Institute of Technology,
Melbourne, Victoria, Australia

⁽³⁾School of Chemistry, Bristol University, Bristol, BS8 1TS, United Kingdom

⁽⁴⁾Department of Physics, Oklahoma State University, Stillwater, Oklahoma 74078

(Received 23 June 1989)

We report light-scattering measurements of powder diffraction patterns of crystals of essentially hard colloidal spheres. These are consistent with structures formed by stacking close-packed planes of particles in a sequence of permitted lateral positions, A, B, C , which shows a high degree of randomness. Crystals grown slowly, while still containing many stacking faults, show a tendency towards face-centered-cubic packing; possible explanations for this observation are discussed.

PACS numbers: 61.50.Em, 61.70.Ph, 82.70.Dd

Assemblies of hard spheres play an important role in statistical physics as models for simple liquids and because they constitute what is probably the simplest system to show a freezing-melting transition.¹ It is perhaps surprising therefore that the structure of a crystal of hard spheres does not appear to have been established unambiguously. Here we report a study by "powder" light crystallography of the structure of crystals formed by essentially hard colloidal spheres. First we describe the experiments and their interpretation; we then discuss the results, their relevance, and connections with other work.

The particles consisted of poly-methylmethacrylate cores stabilized sterically by thin (~ 15 -nm) layers of poly-12-hydroxystearic acid.² They were suspended in a mixture of decalin and carbon disulfide in proportion chosen to match (nearly) their refractive index (~ 1.51). This provided nearly transparent samples which nevertheless showed quite strong single scattering of light. The particles were the same as those used in a study of the glass transition,³ having mean radius about 170 nm and polydispersity [(standard deviation of the particle size distribution)/mean] of $\lesssim 0.05$.⁴ Effective hard-sphere volume fractions ϕ [(volume occupied by the composite particles)/(total sample volume)] were calculated by procedures described previously.^{3,5,6}

With increasing ϕ suspensions of this type show the phase behavior expected for hard spheres^{3,5,6} (and determined largely from computer studies^{7,8}). For $\phi < \phi_F = 0.494$, the freezing concentration, the equilibrium state is a colloidal fluid. For $\phi > \phi_M = 0.545$, the melting concentration, the equilibrium state is crystalline. At $\phi = \phi_G \approx 0.58$ a glass transition intervenes so that for $\phi > \phi_G$ a long-lived amorphous phase is formed. Colloidal crystals are weak;⁹ slow tumbling of the samples readily "shear melts" any crystals present to form reproducible metastable fluid phases. Then, when left undisturbed, samples in the concentration range $\phi_F < \phi < \phi_G$

recrystallize. Crystallization is nucleated homogeneously¹⁰ at random sites throughout the samples and small crystallites of size in the range 10–50 μm are formed. For $\phi_F < \phi < \phi_M$ gravitational settling of the crystallites leads to coexisting colloidal fluid ($\phi = \phi_F$) and crystalline ($\phi = \phi_M$) phases separated by clearly visible boundaries.⁵ For $\phi_M < \phi < \phi_G$ the samples become completely filled with crystallites.

The rate of crystal nucleation and growth is determined by competition between the thermodynamic driving force and viscous or frictional effects,¹¹ both of which increase with ϕ . A maximum crystallization rate is found which, in our system, occurs at $\phi \approx \phi_M$.⁶ In a sample at this concentration crystallization is essentially complete in 1 h. By contrast at $\phi \approx \phi_F$, where the driving force is small, and at $\phi \approx \phi_G$, where particle diffusion is slow, complete crystallization can take several days.

In this system the naturally occurring crystallization process provides samples containing many ($> 10^6$ cm^{-3}) randomly oriented crystallites, which are ideal for the light-scattering equivalent of powder crystallography. To make the measurements, the beam of a Kr^+ ion laser was expanded and passed through a rectangular aperture so that a volume of the sample of order 1 cm^3 was illuminated. The 1-cm^2 square-cross-section sample cell was placed on the axis of a cylindrical bath containing liquid which matched the refractive indices of the suspension (closely) and of the glass sample cell (approximately). Parallel scattered light was focused by the bath, acting as a cylindrical lens, onto a vertical slit which preceded a diffuser and a photomultiplier-tube detector. These detection optics were mounted on an arm which rotated, under computer control, about the bath axis. Scans over scattering angles from 20° to 140° in steps of 0.25° (roughly the angular resolution of the optics) took about 10 min.

For orientationally invariant materials such as fluids or a powder of crystallites the intensity of scattered light

$I(Q)$ can be written as $I(Q) \propto P(Q)S(Q)$; here Q is the scattering vector, $P(Q)$ is the single-particle form factor (determined by the refractive-index profile of the particles), and $S(Q)$ is the structure factor. Form factors were determined, as described elsewhere,⁶ by measurements of $I(Q)$ on dilute suspensions [for which $S(Q) = 1$]. Structure factors, in arbitrary units, were obtained by measuring $I(Q)$ for the concentrated suspensions and dividing by the appropriate form factors. A typical form factor is shown in Fig. 1(a); it has a shape similar to that expected for a particle with a spherically symmetrical core-shell refractive-index profile. Because of the deep minimum near $Q = 3 \times 10^5 \text{ cm}^{-1}$, structure-factor data become unreliable in this region of Q .

Figure 1(b) shows measurements of structure factors of a sample at $\phi = 0.535$, just below the melting concentration,¹² where crystallization is rapid. The lower curve is for the metastable fluid obtained immediately after shear melting the sample by slow tumbling. The upper curve was measured about 1 h later, when crystallization appeared to be complete, and is of a rather unusual form for a crystal. A sharp Bragg reflection is evident, but also a broad, structured band of diffuse scattering.

To analyze this finding we speculate on possible structures. It is generally expected that the crystal structure of spheres with short-ranged isotropic interactions should be close packed. Close-packed structures may be formed by the stacking of hexagonally close-packed layers of particles.^{13,14} Each layer can adopt one of three lateral

positions, A , the reference position, B , obtained by a translation $\mathbf{a}/3 + 2\mathbf{b}/3$ relative to A , and C , obtained by displacement $2\mathbf{a}/3 + \mathbf{b}/3$, where \mathbf{a} and \mathbf{b} are (hexagonal) lattice vectors in layers. The sequence $\dots ABABAB \dots$ gives a hexagonal close-packed (hcp) structure, whereas $\dots ABCABC \dots$ corresponds to face-centered cubic (fcc). However, the only essential requirement for close packing is that adjacent layers, n and $n+1$, have different positions. In the case of hard spheres there seems no reason to expect much "communication" between layers n and $n+2$. Thus we postulate that a hard-sphere crystal may adopt a "random" stacking sequence such as $\dots ABCBCACB \dots$ ¹⁵ For generality we assign a probability α that layers n and $n+2$ have different positions. Then $\alpha = 0$ gives hcp and $\alpha = 1$, fcc.

Calculation of the powder diffraction pattern of a crystal comprises two operations, determination of its reciprocal-space structure and orientational averaging. For a close-packed random-stacked (in the sense described above) crystal the former was worked out many years ago by Wilson,¹³ using finite-difference equations, and by Hendricks and Teller,¹⁶ using correlation-probability matrices. We take the third lattice vector \mathbf{c} to be perpendicular to the close-packed planes and to have a length equal to the interplanar spacing¹⁴ (this is one-half of the length usually used to index an hcp crystal). Then, intensity is found in reciprocal space only along the hexagonally arranged $\{hk\}$ lines. If $(h-k)/3$ is integral, the intensity appears as points which give rise

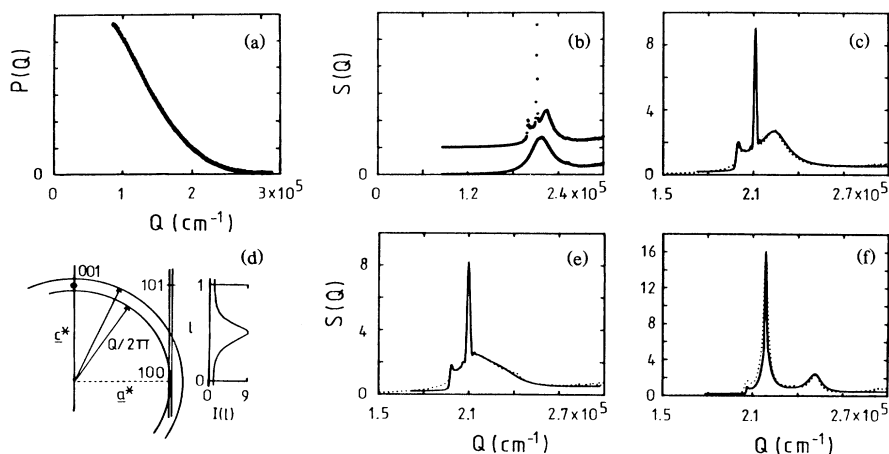


FIG. 1. (a) Typical measured form factor $P(Q)$ (Q is scattering vector) for the particles of radius 170 nm. (b) Structure factors $S(Q)$, in arbitrary units, for a sample just below the melting concentration: lower curve, metastable fluid; upper curve (shifted up one division for clarity), polycrystal. (c) Comparison of crystal data from (b) with theory for completely random stacking (stacking probability $\alpha = 0.5$). (d) Section of reciprocal space in $(\mathbf{a}^*, \mathbf{c}^*)$ plane showing $00l$ line and one of the six $\{10l\}$ lines. The plot at the right-hand side shows the distribution of intensity $I(l)$ along the $10l$ line for $\alpha = 0.5$. Spheres (circles) are drawn for scattering vectors Q corresponding to the "prepeak" at $Q \approx 2 \times 10^5 \text{ cm}^{-1}$ and the maximum at $Q \approx 2.25 \times 10^5 \text{ cm}^{-1}$ in (c). Note the large area of intersection of the smaller sphere with the diffraction-broadened $10l$ rod near reciprocal-lattice point 100. (e) Structure factor of crystalline phase of sample in coexistence region; theory has $\alpha = 0.58$. (f) Structure factor of "sedimentary" crystal (see text); theory has $\alpha = 0.8$. In (c), (e), and (f) dotted lines are experiment, and solid lines are theory.

to those Bragg reflections common to both perfect fcc and perfect hcp structures. If $(h-k)/3$ is not integral, the intensity varies continuously with index l along the lines $\{hk\}$ in a manner determined by the stacking probability α . For $\alpha=0.5$ the relative intensity oscillates between 1 at $2l$ even and 9 at $2l$ odd.¹⁴ A section of reciprocal space in the plane of the reciprocal-lattice vectors \mathbf{a}^* and \mathbf{c}^* is shown in Fig. 1(d). The finite size of a real crystal broadens the points into nodes and the lines into rods.^{14,17} Orientational averaging may be achieved by considering a sphere of radius $Q/2\pi$ centered in reciprocal space^{13,14,17} [see Fig. 1(d)]. Contributions to the real-space powder intensity are proportional to the product of the fraction of the area of the sphere surface which intersects a feature in reciprocal space and the intensity of the feature.

We have calculated powder patterns using the expressions of Wilson¹³ and the orientational-averaging procedure described by Brindley and Méring.¹⁷ As adjustable parameters we need an overall scaling factor, the average crystallite dimensions in the \mathbf{a} and \mathbf{b} directions (assumed to be the same and typically found to be $\sim 25 \mu\text{m}$) and the \mathbf{c} direction (typical value $\sim 15 \mu\text{m}$), and the stacking probability α . To account for the Brownian motions of the particles, thermal diffuse scattering was included.¹⁴ We assumed an Einstein (independent oscillator) model with root-mean-square displacement of a particle about its lattice site equal to 13% of the mean interparticle spacing.¹⁸ The slight disagreement between experiment and theory observed at small values of Q in Figs. 1(c) and 1(e) probably reflects the neglect, in this simple model, of correlations between the displacements of different particles.

Figure 1(c) shows the data of Fig. 1(b) compared with the theoretical curve for $\alpha=0.5$. The features in this pattern may be understood by reference to Fig. 1(d). As the radius of the sphere is increased from $Q=0$, intensity is first obtained on intersection of the six diffraction-broadened $\{10\}$ rods at $l \approx 0$. The "prepeak" in the diffuse scattering of Fig. 1(b) results from the large area of this first intersection and not from a maximum of the intensity in reciprocal space. On further increase of Q the Bragg reflections $\{00\}$ are obtained from the $00l$ line. These correspond to the main reflections from the close-packed planes [one set of (111) planes in the usual fcc indexing]; since, for these reflections, the scattering vector \mathbf{Q} is perpendicular to the planes, the sequence of lateral positions is irrelevant. The subsequent maximum in the diffuse scattering results from the maxima at $l = \pm \frac{1}{2}$ on the $\{10\}$ rods.

Agreement between the experimental data of Fig. 1(c) and the theory with $\alpha=0.5$ is good. Figure 1(e) shows the data for the crystalline phase of a more dilute sample at volume fraction $\phi=0.523$ in the coexistence region. This sample took about 1 day for complete crystallization and phase separation. The high- Q maximum in the

diffuse scattering is now absent implying a redistribution of intensity along the $\{10\}$ lines in reciprocal space. Again the data can be described well by theory, now with a stacking probability $\alpha=0.58$ which indicates a slight preference for local sequences for fcc stacking. Figure 1(f) shows data for a crystal grown by a mechanism not mentioned hitherto. A relatively dilute sample, $\phi \approx 0.25$, was left undisturbed for several weeks. On slow gravitational settling of the particles, crystals grew from the bottom of the cell. These data can be fitted roughly by the theory with $\alpha=0.8$. The incipient 200 line of the fcc structure [$10\frac{2}{3}$ in the indexing of Fig. 1(d)] is clearly evident at $Q \approx 2.5 \times 10^5 \text{ cm}^{-1}$.

Thus there appears to be a correlation between structure and the rate at which the crystals have grown. For crystals which grow at the maximum rate the stacking is essentially completely random, $\alpha=0.5$. We expect this finding to be generic for hard spheres: It is difficult to imagine a mechanism by which such a completely random stacking would be influenced by minor departures of the interparticle potential from the hard-sphere form, for example, slight softness or attraction,^{5,6} or by a small polydispersity. However, such factors could be responsible for the tendency towards the fcc structure, $\alpha > 0.5$, observed in crystals grown at lower concentrations where, under the influence of a smaller "supersaturation," the particles presumably have more time to explore possible lattice sites. On the other hand, it may be that the true equilibrium structure of hard-sphere crystals is fcc, but that the difference in free energies between this and other structures is very small. In fact, several calculations¹⁹ have indicated that the free energies (per particle) of fcc and hcp hard-sphere crystals are the same within an uncertainty of no more than $\sim 2 \times 10^{-3} k_B T$. Thus long-lived nonequilibrium states are easily achieved. Nonequilibrium hydrodynamic interactions (on settling) or macroscopic shear deformations²⁰ may favor the formation of certain structures which will persist and be hard to distinguish from true equilibrium states. Clearly to test these conjectures will require a very detailed study of the interparticle interaction and a more quantitative analysis of the nucleation and growth processes.

Most atomic materials which crystallize into close-packed structures choose either essentially perfect hcp or fcc. Occasionally a significant fraction of stacking faults is found, particularly near a structural phase transition. In fact, Wilson¹³ developed his theory to explain x-ray diffraction measurements on predominantly hcp cobalt: These data²¹ could be explained by random stacking with $\alpha \approx 0.1$, i.e., on average one fault every ten planes. To our knowledge no simple atomic system shows the complete randomness in stacking, $\alpha=0.5$, found in the present work.

Random stacking of colloidal spheres was discussed previously by Sanders²² in connection with gem opals, which consist of solidified arrays of silica particles

formed from aqueous suspension. Sanders showed that the diffuse scattering associated with the stacking disorder is an important factor determining the gem quality, the beautiful coloration observed when opals are illuminated by white light. However, he was not able to obtain from these naturally occurring materials powder diffraction patterns, such as those of Fig. 1, suitable for quantitative analysis.

Two of us (P.N.P. and W.v.M.) acknowledge valuable discussions with the late J. V. Sanders. One of us (B.J.A.) acknowledges support by the Department of Energy under Grant No. DE/FG05/88ER/54349.

¹See, for example, J. P. Hansen and I. R. McDonald, *Theory of Simple Liquids* (Academic, New York, 1976).

²L. Antl, J. W. Goodwin, R. D. Hill, R. H. Ottewill, S. M. Owens, S. Papworth, and J. A. Waters, *Colloid. Surf.* **17**, 67 (1986).

³P. N. Pusey and W. van Meegen, *Phys. Rev. Lett.* **59**, 2083 (1987).

⁴This polydispersity, $\lesssim 0.05$, is significantly smaller than the critical value, $\gtrsim 0.065$, above which the crystallization of hard spheres starts to be suppressed; see P. N. Pusey, *J. Phys. (Paris)* **48**, 709 (1987).

⁵P. N. Pusey and W. van Meegen, *Nature (London)* **320**, 340 (1986); photographs showing the phase behavior of hard-sphere colloids are published here.

⁶P. N. Pusey and W. van Meegen, in *Physics of Complex and Supermolecular Fluids*, edited by S. A. Safran and N. A. Clark (Wiley, New York, 1987).

⁷W. G. Hoover and F. H. Ree, *J. Chem. Phys.* **49**, 3609 (1968).

⁸L. V. Woodcock, *Ann. N.Y. Acad. Sci.* **37**, 274 (1981).

⁹B. J. Ackerson and N. A. Clark, *Phys. Rev. Lett.* **46**, 123 (1981); H. M. Lindsay and P. M. Chaikin, *J. Chem. Phys.* **76**, 3774 (1982).

¹⁰The claim that the crystallization is homogeneously nucleated is supported by the observations that the crystallites are compact and the density of nuclei increases with particle concentration. Heterogeneous nucleation at the cell walls has been observed at high concentration, $\phi \approx \phi_G$, and leads to large crystallites having irregular morphologies (Ref. 5).

¹¹See, for example, R. F. Strickland-Constable, *Kinetics and Mechanism of Crystallization* (Academic, London, 1968).

¹²For reasons not established these samples showed a slightly lower melting concentration, $\phi_M \approx 0.537$, than that, 0.545, found in computer studies (Ref. 7) of hard spheres.

¹³A. J. C. Wilson, *Proc. Roy. Soc. London A* **180**, 277 (1942); *X-Ray Optics* (Methuen, London, 1949).

¹⁴A. Guinier, *X-Ray Diffraction* (Freeman, New York, 1963).

¹⁵J. G. Kirkwood, E. K. Maun, and B. J. Alder, *J. Chem. Phys.* **18**, 1040 (1950).

¹⁶S. Hendricks and E. Teller, *J. Chem. Phys.* **10**, 147 (1942).

¹⁷G. W. Brindley and J. Méring, *Acta Crystallogr.* **4**, 441 (1951).

¹⁸D. A. Young and B. J. Alder, *J. Chem. Phys.* **60**, 1254 (1974).

¹⁹D. Frenkel and A. J. C. Ladd, *J. Chem. Phys.* **81**, 3188 (1984); J. L. Colot and M. Baus, *Mol. Phys.* **56**, 807 (1985); F. Igloi, *J. Phys. C* **19**, 6907 (1986).

²⁰B. J. Ackerson and P. N. Pusey, *Phys. Rev. Lett.* **61**, 1033 (1988).

²¹O. S. Edwards and H. Lipson, *Proc. Roy. Soc. London A* **180**, 268 (1942).

²²J. V. Sanders, *Acta Crystallogr. Sect. A* **24**, 427 (1968).